Binding Specificities of Nanobody•Membrane Protein Complexes Obtained from Chemical Cross-Linking and High-Mass MALDI Mass Spectrometry

Author(s):
Köhler, Martin; Neff, Christoph; Perez, Camilo; Brunner, Cyrill; Pardon, Els; Steyaert, Jan; Schneider, Gisbert; Locher, Kaspar P.; Zenobi, Renato

Publication date:
2018-04-17

Permanent link:
https://doi.org/10.3929/ethz-b-000255257

Originally published in:
Analytical Chemistry 90(08), https://doi.org/10.1021/acs.analchem.8b00236

Funding acknowledgement:
166672 - Structural and mechanistic studies of components of bacterial protein N-glycosylation pathway and of vitamin B12 transport (SNF)

Binding Specificities of Nanobody•Membrane Protein Complexes obtained from Chemical Cross-linking and High-Mass MALDI Mass Spectrometry

Martin Köhler,[†] Christoph Neff,[†] Camilo Perez,[‡,§] Cyrill Brunner,[†] Els Pardon,[#,″] Jan Steyaert,[#,″] Gisbert Schneider,[†] Kaspar P. Locher,[‡] and Renato Zenobi *[,†]

[†]Department of Chemistry and Applied Biosciences, ETH Zürich, Vladimir-Prelog-Weg 3, 8093 Zurich, Switzerland

[‡]Institute of Molecular Biology and Biophysics, ETH Zürich, Otto-Stern-Weg 5, 8093 Zurich, Switzerland

[#]VIB-VUB Center for Structural Biology, VIB, Pleinlaan 2, 1050 Brussels, Belgium

″Structural Biology Brussels, Vrije Universiteit Brussel, Pleinlaan 2, 1050 Brussels, Belgium

ABSTRACT: The application of nanobodies as binding partners for structure stabilization in protein x-ray crystallography is taking an increasingly important role in structural biology. However, the addition of nanobodies to the crystallization matrices might complicate the optimization of the crystallization process, which is why analytical techniques to screen and characterize suitable nanobodies are useful. Here, we show how chemical cross-linking combined with high-mass matrix-assisted laser/desorption ionization mass spectrometry can be employed as a fast screening technique to determine binding specificities of intact nanobody•membrane protein complexes. Titration series were performed to rank the binding affinity of the interacting nanobodies. Microscale thermophoresis was used to validate the mass spectrometry data, which show binding affinities of the stronger binding nanobodies, in the low µM range. In addition, mass spectrometry provides access to the stoichiometry of the complexes formed, which enables the definition of conditions under which homogenous complex states are present in solution. Conformational changes of the membrane protein were investigated and competitive binding experiments were used to delimit the interaction sites of the nanobodies, which is in agreement with crystal structures obtained. The results show the diversity of specifically binding nanobodies in terms of binding affinity, stoichiometry and binding site, which illustrates the need for an analytical screening approach.

In recent years, there has been a growing interest in nanobody-assisted structure determination in x-ray crystallography. Many structures have been solved using nanobodies (Nbs) as protein structure stabilizers, including multi-protein assemblies[1-3], transient protein conformations[4-6] and membrane proteins[7,8]. Nbs are single-domain heavy chain antibodies found in camelids and sharks, and show attractive characteristics in terms of protein crystallization due to high stability and affinity, high solubility and specificity. In addition, their small size (12-15 kDa) also allows interaction with cavities of target proteins that are inaccessible for more commonly used antibodies, which are much larger (~150 kDa)[9]. However, a common problem in protein crystallography is the heterogeneity of protein complexes formed in solution[10], specifically in terms of stoichiometries. In case of Nb assisted protein crystallization, the heterogeneity could be induced by nanobodies, which interact with a low affinity or low selectivity and are therefore unable to sufficiently stabilize the target protein. Therefore, Nbs as protein chaperons have to be selected carefully. This is why different analytical methods are applied to screen and characterize suitable Nbs, including chromatographic methods[11] or surface plasmon resonance spectroscopy[12]. However, these techniques are limited to information about the interaction specificities and are often time consuming, which makes them unsuitable for high-throughput measurements.

The application of mass spectrometry (MS) in the field of structural biology as a tool for high-throughput screening and investigation of binding specificities is becoming more important. The capability of electrospray ionization (ESI) MS to maintain non-covalent interactions intact enables the characterization of protein complexes via MS including the *E. coli* vitamin B_{12} transporter complex $BtuC_2D_2$[13] or the large membrane protein complex V-type

ATPase[14]. In this context, MS can be used not only to obtain the accurate mass of a protein and the folded complexes, but it also provides insight into the stoichiometric distribution[15] of the interacting proteins within a complex. Furthermore, MS-based methods have enabled the detection of conformational changes using ion mobility separation[16], and the determination of dissociation constants for different protein•ligand complexes[17,18]. Therefore, MS has become an important technique in structural biology and pharmaceutical research. A disadvantage of ESI-MS is the requirement for MS-compatible buffers, special detergents or amphipols, and also the limited availability of specialized instruments, which are able to release the trapped proteins into the gas phase and transmit high m/z ions[19].

Beside ESI MS, matrix-assisted laser desorption ionization (MALDI) MS is also used to characterize protein complexes. Due to the acidic character of many MALDI matrices and the disruption of complexes during ion formation, non-covalent interactions need to be stabilized by chemical cross-linking in solution prior to analysis. MALDI-MS is characterized by a high tolerance against salts and detergents in the analyte solution. This allows direct investigation of membrane proteins without the need for laborious buffer and detergent exchange (or removal) prior to MS analysis, which reduces the analysis time. In addition, MALDI can also be used to investigate the binding behavior in the presence of cofactors or ligands that induce conformational changes in the target proteins, which in turn may affect their interaction with binding partners. However, commercially available instruments are usually only able to detect comparatively low MWs (up to 50 kDa) with reasonable signal intensities, which is disadvantageous for protein complex analysis. Here, we use MALDI-MS combined with a high-mass detector, which relies on the production of secondary ions by the impact of the primary ions. This detector has been shown to be more sensitive to higher MWs than the more conventional microchannel plate detector[20]. Therefore, we are able to characterize the stoichiometric distribution of large protein complexes (up to 1.5 MDa).

In this study, we use chemical cross-linking combined with high-mass MALDI-MS as a fast screening and characterization technique of interacting proteins. We studied the ATP-binding cassette (ABC) transporter PglK in complex with different nanobodies (Nbs). PglK is a homodimeric membrane protein composed of a transmembrane (green colored protein structure, **Figure 1**) and nucleotide binding domain (blue colored protein structure), and has ATPase activity. The protein is involved in the N-glycosylation pathway of Campylobacter jejuni by flipping a lipid-linked oligosaccharide from the cytoplasmic side of the membrane into the periplasm[21]. The translocation of the substrate is realized by conformational changes

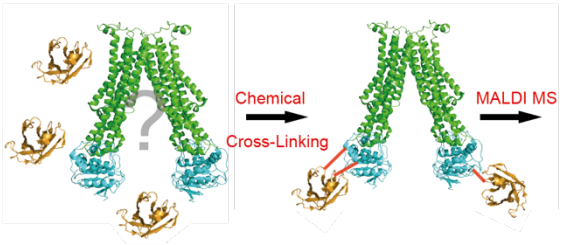

Figure 1. The homodimeric ABC-transporter PglK (PDB: 5C76) consists of a transmembrane (green) and a nucleotide-binding domain (blue) and interacts with certain produced nanobodies (brown, for illustration PDB: 1I3V was used) that are able to stabilize the tertiary structure of the protein. In our study, we used chemical cross-linking combined with high-mass MALDI mass spectrometry to directly access the intact protein complexes formed.

of PglK, which result from the release of energy during ATP hydrolysis (**Figure 4**). To stabilize the structure of PglK or certain intermediate conformations, Nbs were discovered, expressed and the resulting Nb•PglK complexes characterized using cross-linking and high-mass MALDI-MS. We obtained information about binding specificities and demonstrated the diversity of the binding characteristics of different Nbs. These results were validated by microscale thermophoresis and x-ray crystallography analysis.

Experimental Section

PglK expression and purification. PglK and the mutant PglK-E510Q were expressed and purified according to the procedure described by Perez *et al*.[5]. Briefly, N-terminal His_6 tagged PglK from *C. jejuni* and the mutant PglK-E510Q (reduced ATPase activity) were overexpressed in *E. coli.* The cells obtained were harvested by centrifugation, resuspended and disrupted. Membranes were pelleted by ultracentrifugation and PglK was solubilized. NiNTA affinity and size exclusion chromatography were used to purify the membrane protein.

Nanobody discovery, expression and purification. The production of the specific binding Nbs (Nb84, Nb87, Nb93, Nb67, Nb80 and Nb97) and the control Nb (targets PglB) was performed according to the method of Pardon *et al*.[22]. The expression and purification of the Nbs was published earlier by Perez *et al*.[5]. Briefly, Nbs were expressed in *E. coli*. The bacteria cells were pelleted, resuspended and osmotically lysed. After centrifugation, the supernatant was initially purified via Ni-NTA resin followed by gel filtration.

PglK•Nb93 crystallization. A functional PglK mutant E510Q[23] was purified, followed by incubation with purified Nb93 at molar ratios ranging from 1:1 to 1:3 PglK-homodimer:Nb93. The PglK-E510Q•Nb93 complex was concentrated to 8-10 mg/ml in an Amicon Ultra-15 concentrator (Millipore) with a molecular mass cutoff of 100 kDa. The protein was crystallized by vapor diffusion in sitting drops or hanging drops at 20ºC against reservoir containing 100 Glycine pH 9.4; 1 M NaCl; 25% PEG400. The protein to reservoir volume ratio was 2:1 to 1:1. Crystals typically appeared after 3 to 4 days and matured to full size within 2 weeks. Crystals were cryoprotected by gently increasing the cryoprotectant concentration in the drops (up to 30% PEG400) and directly flash frozen by immersion in liquid nitrogen before data collection.

Data collection. Crystals belonged to the space group $P2_12_12_1$ with the following unit cell dimensions: a=151.77 Å, b=172.09 Å, c=210.30 Å. Diffraction data was collected at the beamline X06SA at the Swiss Light Source (SLS, Villigen). Data were processed and merged with XDS[24] and anisotropic scaling/ellipsoid truncation was performed using the UCLA diffraction anisotropy server[25]. The resolution limits along a*, b* and c* were 7.1 Å, 6.8 Å and 6.8 Å respectively, which correspond to mild anisotropic data.

Structure determination. The structure was determined by molecular replacement with a modified model of a PglK-E510Q structure determined previously at 2.9 Å (PDB code 5C78)[23], and a homology model of Nb93. Molecular replacement was performed using the program Phaser[26], refinement was performed using Phenix[27] combined with manual building in Coot[28].

Titration of PglK against nanobodies. 18 µM PglK solution (monomer concentration in 10 mM HEPES, 150 mM NaCl, 0.02 % LMNG, pH 8.0) was titrated against 2.25, 4.5, 9, 18, 27 and 45 µM Nb solution (in 10 mM HEPES, 150 mM NaCl, pH 8.0, respectively, using a volume ratio of 1:1. After an incubation time of 10 min on ice, the cross-linking reaction was performed using 0.1 % (v/v) glutaraldehyde for 30 min. To improve the quality of the mass spectrometric signals, the samples were washed using ultra-centrifugal filters (0.5 mL, NMWL of 100 kDa) from Merck Millipore at 8000 x g for 15 min at 4°C. After 5 washing cycles with 100 µL PglK buffer solution, respectively, the excess of Nbs and cross-linking reagent was removed.

Influence of nucleotides on complex formation. 18 µM PglK-E510Q (monomer concentration in 10 mM HEPES, 100 mM NaCl, 0.016 % LMNG, pH 7.5) were incubated in 5 mM $MgCl_2$ and 5 mM ADP or ATP, respectively, for 5 min on ice. In a next step the solution was mixed with 18 µM of different Nbs for 10 min on ice using a volume ratio of 1:1. The cross-linking reaction and sample preparation were carried out prior to mass spectrometric analysis (described previously).

Localization of the binding site by incubating two different nanobodies. 18 µM PglK were incubated with 18 µM Nb87 or Nb84 for 10 min on ice followed by the addition of 18 µM of a different Nb (Nb93, Nb67, Nb80 or Nb97). The

reference spectrum was obtained by incubating 18 µM PglK with 36 µM Nb87 or Nb84, respectively. The cross-linking reaction and sample preparation were performed prior mass spectrometric analysis.

Mass spectrometry. The samples were spotted on a stainless steel MALDI target plate using a sandwich spotting technique (three layers: matrix-sample-matrix, 0.5 µL each layer). Sinapic acid (10 mg/mL in acetonitrile/water/TFA, 49.95/49.95/0.1, v/v/v) was used as the MALDI matrix. All mass spectrometric measurements were performed in positive linear ion mode on a commercial MALDI-TOF/TOF mass spectrometer (ABI 4800, AB Sciex) equipped with a high-mass detector (HM2, CovalX). The high voltages 1 and 2 of the HM2 detector were set to – 3.6 kV and – 20 kV, respectively. MALDI was initiated using a pulse from a Nd:YAG laser (355 nm), and 500 shots per spectrum were accumulated. The best signal quality was obtained using a grid to source 1 ratio of 0.99 and a delay time of 1800 ns. Every spectrum was recorded in a mass range from m/z 5000 to 1000000 with a focused mass of m/z 140000. The data obtained were smoothed (Savitzky-Golay) using Igor Pro (version 6.37, WaveMetrics, USA).

Protein labeling for microscale thermophoresis. PglK was diluted to 5 µM to a total volume of 100 µl, mixed with 100 µl of 15 µM dye RED-NHS (NanoTemper) and incubated for 30 minutes at room temperature. The labeling was performed in the assay buffer. Unreacted dye was eliminated by gravity flow-guided size exclusion chromatography with a PD-10 desalting column.

Microscale thermophoresis. All measurements were performed with a 1:1 serial dilution of the investigated nanobodies to yield 10 µl of each concentration. 10 µl of labeled protein were added randomly to each Nb dilution series for a final labeled protein concentration of 500 pM. The measurements were performed on a Monolith NT.115Pico instrument (NanoTemper) with premium coated capillaries. Excitation power was set at 40-60% to yield 4000-8000 counts, MST-power to 40% with a laser-on time of 20 s and a laser-off time of 3 s. Temperature was set to 25°C. Each measurement was performed in three replicates. The data was analyzed by the MO Affinity Analysis software. Due to ligand-induced fluorescence changes in all samples, the initial fluorescence was considered for fitting and the K_D was determined using Eq. 1. "Unbound" and "bound" refer to the fluorescence signal at the lowest and highest concentration of the measured ligand, respectively; "c" and "c_{Tar}" refer to the concentrations of ligand and target, respectively.

(1) $$f(c) = Unbound + \frac{(Bound-Unbound)\times(c+c_{Tar}+K_d-\sqrt{(c+c_{Tar}+K_d)^2-4\times c\times c_{Tar}}}{2\times c_{Tar}}$$

Results and Discussion

Cross-linking strategy. In this study, we applied chemical cross-linking combined with high-mass MALDI-MS to characterize intact Nb•membrane protein complexes. This analytical method allows one to obtain direct insight into the stoichiometric distribution of complexes formed in solution. To keep the protein complexes intact during MALDI-MS measurements, a suitable cross-linking strategy is required. The cross-linker should react very efficiently with functional amino acid residues of the interacting proteins to avoid further time consuming protein complex purification steps, and the spacer length of the cross-linker should be in an optimal range to link binding proteins.

We opted to use the highly reactive cross-linker glutaraldehyde. This aldehyde is characterized by its capability to react with many different amino acids including lysine[29], tyrosine, tryptophan, phenylalanine[30], histidine and cysteine[31]. Therefore, the probability to obtain false negative results induced by a lack of cross-links created between interacting proteins is reduced. A drawback is that glutaraldehyde is known to polymerize in aqueous solution[32], which makes it difficult to determine the exact spacer length. To avoid long polymer chains of glutaraldehyde, which could potentially lead to non-specific cross-links between proteins, we used a low concentration (0.1 % v/v) of glutaraldehyde and short reaction times (30 min) on ice. In addition, a control Nb that targets a structurally completely different protein (PglB) was used to

gauge the amount of non-specific interaction products.

Insights into stoichiometries using MALDI-MS. The homodimeric ABC-transporter PglK consists of a transmembrane domain (green) and the nucleotide binding domain (blue) (**Figure 1**). At high binding selectivity towards Nbs, each membrane protein monomer is able to bind at most one Nb (brown). In the screening study, we investigated five different Nbs (Nb80, Nb84, Nb87, Nb93 and Nb97), which were published earlier by Perez et al.[5] and are known to interact with PglK (pull-down assay, supplementary Figure S1A from Perez et al.[5]) and are characterized by their different influence on the ATPase activity of the ABC-transporter (shown in supplementary Figure 2A from Perez et al.[5], ATPase activity assay).

Figure 2 compares MALDI mass spectra obtained by cross-linking 18 µM PglK with a series of six Nbs, over a range of PglK dimer:Nb molar concentration ratios. At low Nb concentrations all mass spectra show an abundant signal at 142,000 m/z, which corresponds to the bare PglK dimer. By increasing the Nb concentration, signals for PglK in complex with one (157,000 m/z) and two Nbs (172,000 m/z), and a signal for unbound Nb (15,000 m/z), could also be detected.

At the highest Nb concentrations used, Nb84, Nb87 and Nb93 (**Figure 2A–C**) also showed signals for the PglK in complex with up to five Nbs. There could be two reasons for the formation of these complexes: first, the binding specificities of Nb84, Nb87 and Nb93 are not very high and different

Figure 2. Comparison of MALDI-MS experiments obtained by cross-linking 18 µM PglK with a series of six Nbs, over a range of Nb:PglK molar concentration ratios. In the representative mass spectra (left panels), peaks corresponding to unbound PglK (at m/z 142,000), unbound Nb (at m/z 15,000), and bound PglK:Nb species (e.g., 1:1 at m/z 157,000 and 1:2 at m/z 172,000) are labeled. In the titration curves (right panels), the fractional intensities of unbound and Nb-bound PglK species are plotted. At

higher Nb concentrations, all MALDI-MS spectra obtained showed signals for PglK in complex with one Nbs and two Nbs. At the highest Nb concentrations, complexes composed of more than two Nbs were visible. The titration diagrams were obtained from the relative intensities of the peaks in the corresponding spectra. They illustrate the fraction of the different complex formed: bare PglK (blue trace), PglK dimer with one Nb (red trace), with two Nbs (green trace), three Nbs (black trace), with four Nbs (orange trace) and with five Nbs (yellow trace). Nb84, Nb93 and Nb87 showed a strong affinity to create 1:1 and 1:2 PglK (dimer) Nb complexes at low Nb concentration. In contrast, Nb67 and Nb97 showed a low affinity to create complexes, comparable to the control Nb.

affinities may exist. Second, the Nbs could oligomerize at higher concentrations and create complexes with PglK. These transient protein interactions would probably also be stabilized by chemical cross-linking[33] and could lead to the higher complexation states.

To understand the role of transient or nonspecific interactions in our experiments, we performed a titration experiment with the control Nb against PglK (**Figure 2D**). Only at high Nb concentrations, abundant signals for the PglK in complex with one Nb could be found, which illustrates a comparative small influence on the results and can qualitatively be used as nonspecific background interactions. Overall, the results give insight into the stoichiometry of Nb•PglK complexes at different Nb concentrations, which is useful to determine conditions in which a homogenous complex distribution is present in solution (e.g. Nb93 at a molar ratio of 1:1 or 1:2, **Figure 2B**). The data could be used for protein x-ray crystallography, where homogenous protein complex solutions are essential to obtain good quality protein crystals for a high resolution in x-ray studies[10].

Determination of the binding affinity using Microscale thermophoresis. The observed abundant signals in MALDI-MS experiments corresponding to PglK in complex with one and two Nbs at low Nb concentrations suggests that Nb84, Nb87 and Nb93 are strong binders (**Figure 2A–C**). In particular, Nb93 shows very abundant and homogenous complex formation behavior already at a molar ratio of 1:1 (**Figure 2B**). In contrast, Nb67 and Nb97 (**Figure 2E, F**) show a distribution of many different complex species with similar intensities, and PglK in complex with one Nb was the most abundant species only at the highest Nb concentrations used, and the titration curves for these Nbs show a similar behavior in comparison to the control Nb; taken together, this suggests that Nb67 and Nb97 are weakly binding.

We note that comparison of the binding affinity of the protein complexes could only be made under the same conditions (e.g. same matrix, buffer, cross-linker and protein concentrations and same measurement parameters). Quantitative data cannot be obtained due to the lack of information about response factors of the different complexes formed, which are influenced by the ionization efficiency and suppression effects during the MALDI process, the transmission through the time-of-flight analyzer and the detection of the ions. In addition, the crystallization process of the matrix/analyte mixture on the sample plate for MALDI-MS measurements could lead to inhomogeneous crystals, which may also influence the efficiency of the ion formation[34]. Finally, different yields of cross-linked products of different Nbs in complex with PglK could exist, which is depended on the amount and kind of reactive amino acid groups within the interaction site.

To quantitatively determine the binding affinity (K_D) of the Nb•PglK complexes investigated we used microscale thermophoresis (MST) and compared the results with the MALDI-MS data. MST is based on the thermophoretic diffusion of molecules upon application of an IR laser, which produces a temperature gradient. The molecular movement in the temperature gradient is described by the Soret coefficient S_T, which is affected by the size, charge and/or hydration shell of a component (e.g. a protein). Thus, the degree of binding, i.e. to which extent one component is bound by the second (e.g. a protein bound by a ligand), results in a different thermophoretic movement. Fluorescence read-out by labeling one of the interaction partner serves as measurement technique for the

thermophoresis[35,36]. However, covalent labeling with a fluorescent dye can disturb this analysis if the unlabeled component affects the fluorescence properties of the dye[37]. This phenomenon, which is termed ligand-induced fluorescence change, can alternatively be used for analysis[38,39]. The fluorescence of labeled PglK was measured against the investigated set of nanobodies by analysis of initial fluorescence in microscale thermophoresis experiments. All samples showed a ligand-induced fluorescence change.

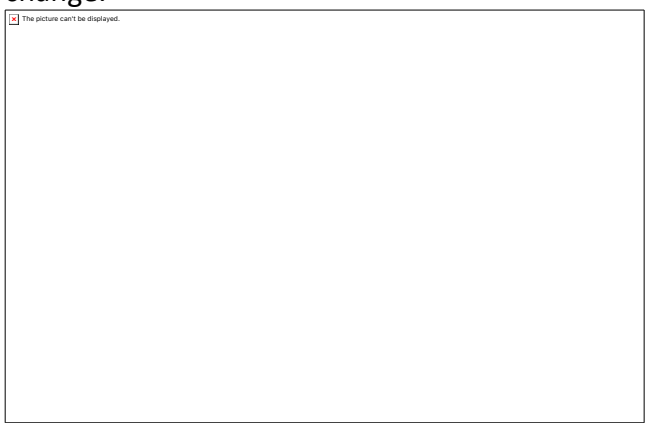

Figure 3. Comparison of microscale thermophoresis titration experiments for Nb84, Nb87, Nb93, Nb97, Nb67 and the control Nb. The derived dissociation constants are listed in the diagram and in **Table S2**. The concentration of labelled PglK was kept constant for these experiments. The Nbs were titrated against PglK. Nb84, Nb93 and Nb87 showed comparatively high binding affinities ranging from 0.5 to 1.8 µM. Control Nb and Nb67 did not show a specific interaction behavior, and Nb97 was determined to bind very weakly with an estimated high K_D value of ca. 140 µM.

The nanobodies Nb84, Nb87, and Nb93 exhibit K_Ds in the range of 0.5 to 1.8 µM. A factor of 2–3 in measured K_Ds is commonly assumed to be the delimiter for measurable differences in biophysical assays, such that we may conclude that these Nbs have similar binding affinities. In contrast, Nb97 was found to have a significantly lower binding affinity, by a factor of ca. 100. Lastly, no binding was observed for Nb67 and control Nb (**Figure 3**). Qualitatively, these results are in good agreement with the MALDI-MS experiments described above (**Figure 2D, E**).

We note that standard MST curves could not be observed for all investigated nanobodies due to ligand-induced fluorescence change for all nanobodies. Ligand-induced fluorescence changes are caused by binding of a ligand close to the labeling side, thus affecting the fluorescence signal. The applied labeling approach by an NHS-ester results in covalent addition of the dye to primary amines. Hence, we might hypothesize that these nanobodies bind at or close to lysine-rich sites.

Influence of nucleotides on Nb•PglK complex formation., The ABC-transporter PglK translocates substrate molecules against a concentration gradient, powered by ATP-induced conformational changes. As illustrated in **Figure 4**, in the presence of ATP, the membrane protein changes its conformation in solution from an apo-inward state to an ADP-bound outward-occluded state. The addition of another ATP molecule leads to the final ATP-bound outward-open state[23].

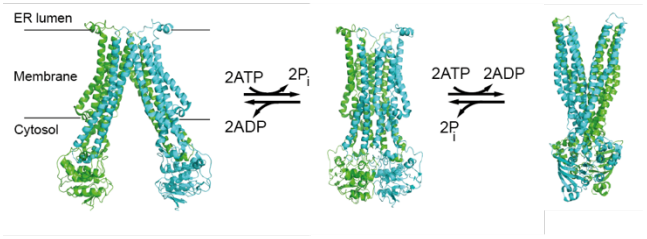

Figure 4. Due to the hydrolysis of ATP, the ABC-transporter PglK changes it conformation from an apo-inward state (PDB: 5C76) to an ADP-bound outward occluded state (PDB: 5C73). The replacement of the ADP molecule with ATP results in an ATP-bound outward-open state (PDB: 2HYD).

We used the different conformations formed in the presence of nucleotides to get insight into the binding site of the Nbs. The Nbs chosen are known to influence the ATPase activity of PglK, as determined using an ATPase activity assay (supplementary Figure 2A from Perez et al.[5]). This can be explained by two effects: either the binding site of the Nb is located near the nucleotide binding site of PglK, resulting in steric hindrance to the binding of nucleotides; or the Nb interacts in the interior of the PglK dimer and

sterically blocks the conformational change. We show here that MALDI-MS can be used to distinguish between these two possibilities and obtain insight into the binding site. PglK was incubated with nucleotides (ADP or ATP, respectively) prior to the addition of the Nbs and to the cross-linking. Due to the hydrolysis of the ATP, PglK may be expected to be present in three different conformations, which are in equilibrium (**Figure 4**). The ADP-bound outward occluded ATP-bound outward-open conformation are characterized by a comparably compact structure and a closed protein interior. If a Nb has a binding site in the interior of PglK, we should observe reduced MS signals from Nb•PglK complexes in the presence of ATP, due to the inaccessibility of the binding site. To be able to observe different complex formation behavior we used the mutant PglK-E510Q, which is characterized by a lower rate of conformational changes due to a reduced ATPase activity[23]. In a previous article, we could already demonstrate the influence of nucleotides on the Nb87•PglK complex. This is shown in **Figure 5A**, which is reproduced here from Perez *et al*.[5] to have the full information: mass spectrometry measurements show a change of signal intensities corresponding to the complexes created from PglK in complex with one Nb87 in the absence of nucleotides (black trace) to the bare protein in presence of ATP (blue trace), which suggests a binding site of Nb87 in between the PglK monomers.

Figure 5 compares results from cross-linking MALDI-MS experiments for Nb87 (A) and Nb93 (B), each in the presence and absence of ATP or ADP. For these experiments, PglK was incubated with nucleotides (ADP or ATP, respectively) prior to the addition of the Nbs and to the cross-linking. For Nb87, the presence of nucleotides reduces the relative abundance of bound PglK•Nb species, whereas for Nb93 the addition of nucleotides appears to have no significant effect. Similar experiments on Nb84, Nb97, control Nb (**Figure S2**) show that these nanobodies behave similarly to Nb93: the addition of nucleotides does not lead to a significant change in the relative abundance of bound to free PglK species.

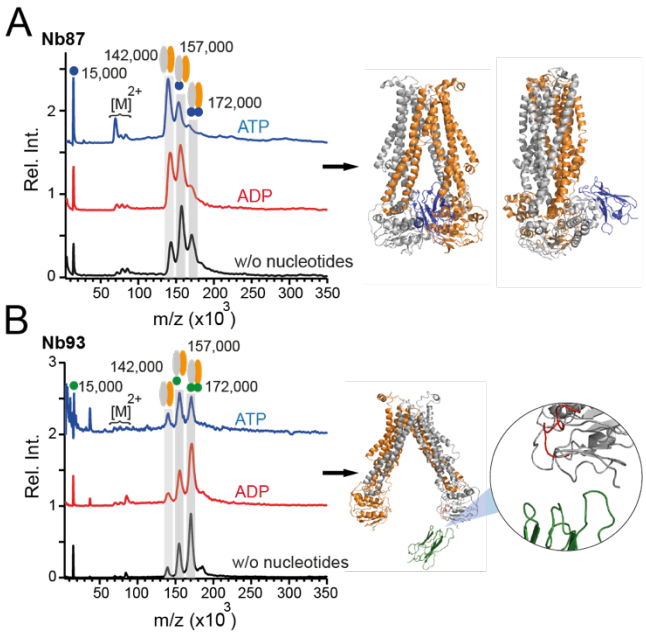

Figure 5. Complex formation of Nb87 and Nb93 was observed in the presence of ADP or ATP, respectively (ADP red trace, ATP blue trace) and compared without nucleotides (black trace). **A** Nb87 showed a significant change in complex formation towards the free PglK, which indicates an interaction of Nb87 in the interior of the homodimer (reproduced from Perez *et al*.[5]). The result was later confirmed with a crystal-structure that shows Nb87 bound to the interspace of the PglK monomers (PglK monomers: grey and orange, Nb87: blue, PDB: 5NBD). **B** A significant change in complex formation using Nb93 was not observed, although it influences the ATPase activity (supplementary Figure 2A from Perez et al.[5]). The crystal structure of PglK in complex with Nb93 shows an interaction site on the exterior of the nucleotide binding domain of PglK.

Overall, these results suggest a unique binding site for Nb87 compared to all other nanobodies examined. This interpretation is supported by results from x-ray studies. The crystal structures of PglK in complex with Nb87 (**Figure 5A**) and Nb93 (**Figure 5B**) show that while both nanobodies are bound to the nucleotide binding domain of PglK, Nb93 leaves the binding site more exposed. Therefore, the complex

formation with Nb93 is less influenced by conformational changes in the presence of nucleotides and a change in the relative abundance of bound to free PglK is not expected via MALDI-MS. Furthermore, in the presence of Nb93, the ATPase activity of PglK is reduced (supplementary Figure 2A from Perez et al.[5]). The crystal structure of the Nb93•PglK complex suggests an interaction site near the ATP binding site of the nucleotide binding domain (**Figure 5B**, binding site is highlighted in red), which may inhibit the binding of ATP and affect its ATPase activity.

Comparison of the binding sites. To characterize the binding sites of each Nb, we simultaneously incubated two different Nbs with PglK (molar ratio of 1:2 for each Nb) prior to chemical cross-linking. Nb87 (**Figure 6A**) and Nb84 (**Figure 6B**), respectively, were used as reference Nbs, and Nb93 and Nb97 were added, respectively. The resulting spectra were compared with the reference Nb•PglK complexes (**Figure 6A and B**, black traces), which were obtained using a molar ratio of 1:4 (PglK dimer to Nb87 or Nb84). Direct comparison of different spectra allowed us to identify Nbs that compete for the same binding site or interact independently with PglK. If two Nbs compete for the same binding site, the spectrum obtained is similar to the reference spectrum (black trace). The competition experiment with Nb87 as reference Nb indicates a binding site that is not shared by Nb93, Nb84 and Nb97 (**Figure 6A**). Indeed, in the presence of Nb93, Nb84 and Nb97, abundant signals for PglK in complex with up to four Nbs could be detected, suggesting independent, noncompetitive binding sites of the Nbs analyzed. In comparison with the reference spectrum of Nb87 (molar ratio of 1:4, **Figure 6A,** black trace), PglK in complex with two Nbs is the most abundant signal. The same

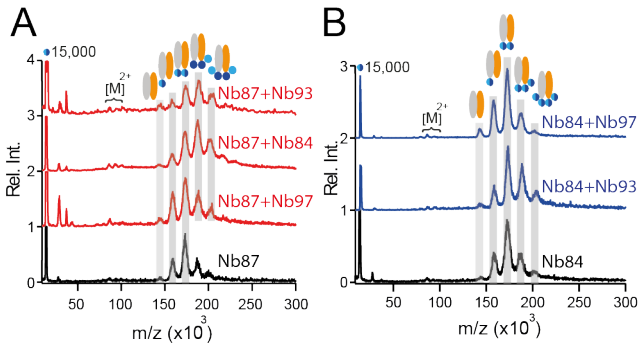

Figure 6. Comparison of the interaction site of Nb87, Nb84, Nb97 and Nb93. **A** Nb87 was incubated with PglK in a 1:2 molar ratio (PglK dimer : Nb) followed by the addition of another Nb again in a molar ratio of 1:2 (PglK dimer : Nb). By comparing the spectra obtained with the reference spectrum of Nb87 in a molar ratio of 1:4 (black trace) we could show that Nb97, Nb84 and Nb93 were not competing for the same binding site (red traces). **B** The same experiment was performed with Nb84. The spectra obtained were similar to the reference spectrum of Nb84. The Nbs used compete for the same binding site.

experiment was repeated with Nb84 as a reference Nb. As explained above, Nb84 binds to another binding site. The spectra obtained using Nb93 and Nb97 in the presence of Nb84 were similar to the reference spectrum, indicating the same binding site. The results from these competition experiments are also in agreement with the crystal structures of PglK in complex with Nb87 and Nb93 that suggest two different binding sites (**Figure 5A and B**). In addition, Nb84, Nb93 and Nb97 showed similar properties (reduced ATPase activity and no influence of ATP on complex formation) in the ATPase activity assay (supplementary Figure 2A from Perez et al.[5]) and the MS measurements of PglK•Nb complexes in presence of nucleotides (**Figure 5 and Figure S2**). The competition experiments further demonstrate that these Nbs share the same binding site, which is close to the binding site of Nb93 as supported by the according crystal structure of the complex (**Figure 5B**).

Conclusions

Chemical cross-linking combined with MALDI-MS is a fast, high-resolution technique for the

screening and characterization of binding specificities of Nb•membrane protein complexes. Due to its high tolerance against salts and detergents, MALDI-MS can be used to directly investigate protein complexes without time-consuming sample preparation steps prior analysis, which are needed for ESI MS. Once the cross-linking reaction is optimized, multiple Nb•membrane protein complexes could be analyzed within a few hours. The direct access to the stoichiometry of the complexes formed provided by MS aids in defining conditions under which homogenous protein complexes are present in solution. In addition, the mass spectrometry data obtained from titration series were used to rank the binding affinity of the interacting Nbs. To quantitatively determine the binding affinities, we used microscale thermophoresis, which confirmed our observations.

In addition, we also could investigate the complex formation in presence of nucleotides, which allowed us to get insight into the binding site of Nb•PglK complexes. The results obtained indicated different binding sites of the Nbs, which were in agreement with crystal structures showing Nb87 and Nb93 in complex with PglK, respectively. Based on these results, Nbs could be used to investigate further intermediate states of protein conformations or structure stabilizing Nbs could be selected, which do not influence the functions of the protein complex. Finally, the mass spectrometry results showed different binding specificities of the Nbs investigated, illustrating the need for screening technique to choose a suitable Nb for different biological systems. This method could be used to optimize the protein crystallization conditions to obtain high-quality crystals for x-ray studies.

ASSOCIATED CONTENT

Supporting Information

The Supporting Information is available free of charge on the ACS Publications website.

Electron density map of PlgK-E510Q•Nb93 complex, MALDI-MS spectra of PglK•Nb complexes in presence of nucleotides and tables relating to MST measurements (PDF)

AUTHOR INFORMATION

Corresponding Author

*Email: zenobi@org.chem.ethz.ch. Tel.: +41 44 632 43 76. Fax: +41 44 632 2 92

Present Addresses

§ Biozentrum University of Basel Klingelbergstrasse 50 / 70, 4056 Basel, Switzerland

E-Mail: camilo.perez@unibas.ch.

Tel.: +41 61 207 59 69

Notes

The authors declare no competing financial interest.

ACKNOWLEDGMENT

The authors thank the Swiss National Science Foundation for financial support of this research (grant # 200020_15929 and # 310030B_166672). We thank Dr. M. Czar and Dr. A. Marchand for the help with manuscript revision. We thank INSTRUCT, part of the European Strategy Forum on Research Infrastructures and the Research Foundation - Flanders (FWO) for their Nanobody discovery support.

REFERENCES

(1) Baranova, E.; Fronzes, R.; Garcia-Pino, A.; Van Gerven, N.; Papapostolou, D.; Pehau-Arnaudet, G.; Pardon, E.; Steyaert, J.; Howorka, S.; Remaut, H. *Nature* **2012**, *487*, 119-122.

(2) Park, Y. J.; Pardon, E.; Wu, M. T.; Steyaert, J.; Hol, W. G. J. *Nucleic acids research* **2012**, *40*, 1828-1840.

(3) Rostislavleva, K.; Soler, N.; Ohashi, Y.; Zhang, L.; Pardon, E.; Burke, J. E.; Masson, G. R.; Johnson, C.; Steyaert, J.; Ktistakis, N. T.; Williams, R. L. *Science* **2015**, *350*, aac7365.

(4) Jiang, X.; Smirnova, I.; Kasho, V.; Wu, J.; Hirata, K.; Ke, M.; Pardon, E.; Steyaert, J.; Yan, N.; Kaback, H. R. *Proceedings of the National Academy of Sciences of the United States of America* **2016**, *113*, 12420-12425.

(5) Perez, C.; Kohler, M.; Janser, D.; Pardon, E.; Steyaert, J.; Zenobi, R.; Locher, K. P. *Sci Rep* **2017**, *7*, 46641.

(6) DeVree, B. T.; Mahoney, J. P.; Velez-Ruiz, G. A.; Rasmussen, S. G. F.; Kuszak, A. J.; Edwald, E.; Fung, J. J.; Manglik, A.; Masureel, M.; Du, Y.;

Matt, R. A.; Pardon, E.; Steyaert, J.; Kobilka, B. K.; Sunahara, R. K. *Nature* **2016**, *535*, 182-186.
(7) Rasmussen, S. G.; Choi, H. J.; Fung, J. J.; Pardon, E.; Casarosa, P.; Chae, P. S.; Devree, B. T.; Rosenbaum, D. M.; Thian, F. S.; Kobilka, T. S.; Schnapp, A.; Konetzki, I.; Sunahara, R. K.; Gellman, S. H.; Pautsch, A.; Steyaert, J.; Weis, W. I.; Kobilka, B. K. *Nature* **2011**, *469*, 175-180.
(8) Rasmussen, S. G.; DeVree, B. T.; Zou, Y.; Kruse, A. C.; Chung, K. Y.; Kobilka, T. S.; Thian, F. S.; Chae, P. S.; Pardon, E.; Calinski, D.; Mathiesen, J. M.; Shah, S. T.; Lyons, J. A.; Caffrey, M.; Gellman, S. H.; Steyaert, J.; Skiniotis, G.; Weis, W. I.; Sunahara, R. K.; Kobilka, B. K. *Nature* **2011**, *477*, 549-555.
(9) Li, J. W.; Xia, L. J.; Su, Y. H.; Liu, H. C.; Xia, X. Q.; Lu, Q. X.; Yang, C. J.; Reheman, K. *J Biol Chem* **2012**, *287*, 13713-13721.
(10) Dessau, M. A.; Modis, Y. *Jove-J Vis Exp* **2011**, *47*.
(11) Wiuf, A.; Kristcnsen, L. H.; Kristensen, O.; Dorosz, J.; Jensen, J.; Gajhede, M. *Acta Crystallogr F* **2015**, *71*, 1235-1241.
(12) Schoonaert, L.; Rue, L.; Roucourt, B.; Timmers, M.; Little, S.; Chavez-Gutierrez, L.; Dewilde, M.; Joyce, P.; Curnock, A.; Weber, P.; Haustraete, J.; Hassanzadeh-Ghassabeh, G.; De Strooper, B.; Van den Bosch, L.; Van Damme, P.; Lemmens, R.; Robberecht, W. *J Biol Chem* **2017**, *292*, 11452-11465.
(13) Barrera, N. P.; Di Bartolo, N.; Booth, P. J.; Robinson, C. V. *Science* **2008**, *321*, 243-246.
(14) Zhou, M.; Morgner, N.; Barrera, N. P.; Politis, A.; Isaacson, S. C.; Matak-Vinkovic, D.; Murata, T.; Bernal, R. A.; Stock, D.; Robinson, C. V. *Science* **2011**, *334*, 380-385.
(15) Smith, V. F.; Schwartz, B. L.; Randall, L. L.; Smith, R. D. *Protein Sci* **1996**, *5*, 488-494.
(16) Wyttenbach, T.; Bowers, M. T. *Annu Rev Phys Chem* **2007**, *58*, 511-533.
(17) Daniel, J. M.; Friess, S. D.; Rajagopalan, S.; Wendt, S.; Zenobi, R. *Int J Mass Spectrom* **2002**, *216*, 1-27.
(18) Tjernberg, A.; Carno, S.; Oliv, F.; Benkestock, K.; Edlund, P. O.; Griffiths, W. J.; Hallen, D. *Analytical chemistry* **2004**, *76*, 4325-4331.
(19) Calabrese, A. N.; Watkinson, T. G.; Henderson, P. J. F.; Radford, S. E.; Ashcroft, A. E. *Analytical chemistry* **2015**, *87*, 1118-1126.
(20) Nazabal, A.; Wenzel, R. J.; Zenobi, R. *Analytical chemistry* **2006**, *78*, 3562-3570.
(21) Alaimo, C.; Catrein, I.; Morf, L.; Marolda, C. L.; Callewaert, N.; Valvano, M. A.; Feldman, M. F.; Aebi, M. *Embo J* **2006**, *25*, 967-976.
(22) Pardon, E.; Laeremans, T.; Triest, S.; Rasmussen, S. G.; Wohlkonig, A.; Ruf, A.; Muyldermans, S.; Hol, W. G.; Kobilka, B. K.; Steyaert, J. *Nat Protoc* **2014**, *9*, 674-693.
(23) Perez, C.; Gerber, S.; Boilevin, J.; Bucher, M.; Darbre, T.; Aebi, M.; Reymond, J. L.; Locher, K. P. *Nature* **2015**, *524*, 433-438.
(24) Kabsch, W. *Acta crystallographica. Section D, Biological crystallography* **2010**, *66*, 125-132.
(25) Strong, M.; Sawaya, M. R.; Wang, S.; Phillips, M.; Cascio, D.; Eisenberg, D. *Proc Natl Acad Sci U S A* **2006**, *103*, 8060-8065.
(26) McCoy, A. J.; Grosse-Kunstleve, R. W.; Adams, P. D.; Winn, M. D.; Storoni, L. C.; Read, R. J. *Journal of applied crystallography* **2007**, *40*, 658-674.
(27) Adams, P. D.; Afonine, P. V.; Bunkoczi, G.; Chen, V. B.; Davis, I. W.; Echols, N.; Headd, J. J.; Hung, L. W.; Kapral, G. J.; Grosse-Kunstleve, R. W.; McCoy, A. J.; Moriarty, N. W.; Oeffner, R.; Read, R. J.; Richardson, D. C.; Richardson, J. S.; Terwilliger, T. C.; Zwart, P. H. *Acta crystallographica. Section D, Biological crystallography* **2010**, *66*, 213-221.
(28) Emsley, P.; Lohkamp, B.; Scott, W. G.; Cowtan, K. *Acta crystallographica. Section D, Biological crystallography* **2010**, *66*, 486-501.
(29) Bowes, J. H.; Cater, C. W. *Biochim Biophys Acta* **1968**, *168*, 341-352.
(30) Hopwood, D.; Allen, C.; McCabe, M. *The Histochemical Journal* **1970**, *2*, 137-150.
(31) Migneault, I.; Dartiguenave, C.; Bertrand, M. J.; Waldron, K. C. *Biotechniques* **2004**, *37*, 790-796, 798-802.
(32) Kawahara, J.-i.; Ishikawa, K.; Uchimaru, T.; Takaya, H. In *Polymer modification*; Springer, 1997, pp 119-131.
(33) Sinz, A. *Mass spectrometry reviews* **2006**, *25*, 663-682.

(34) Wang, C. C.; Lai, Y. H.; Ou, Y. M.; Chang, H. T.; Wang, Y. S. *Philos Trans A Math Phys Eng Sci* **2016**, *374*.
(35) Seidel, S. A.; Wienken, C. J.; Geissler, S.; Jerabek-Willemsen, M.; Duhr, S.; Reiter, A.; Trauner, D.; Braun, D.; Baaske, P. *Angew Chem Int Ed Engl* **2012**, *51*, 10656-10659.
(36) Jerabek-Willemsen, M.; André, T.; Wanner, R.; Roth, H. M.; Duhr, S.; Baaske, P.; Breitsprecher, D. *Journal of Molecular Structure* **2014**, *1077*, 101-113.
(37) Entzian, C.; Schubert, T. *Methods* **2016**, *97*, 27-34.
(38) Zaltariov, M. F.; Hammerstad, M.; Arabshahi, H. J.; Jovanovic, K.; Richter, K. W.; Cazacu, M.; Shova, S.; Balan, M.; Andersen, N. H.; Raduloyic, S.; Reynisson, J.; Andersson, K.; Arion, V. B. *Inorg Chem* **2017**, *56*, 3532-3549.
(39) Muratcioglu, S.; Chavan, T. S.; Freed, B. C.; Jang, H.; Khavrutskii, L.; Freed, R. N.; Dyba, M. A.; Stefanisko, K.; Tarasov, S. G.; Gursoy, A.; Keskin, O.; Tarasova, N. I.; Gaponenko, V.; Nussinov, R. *Structure* **2015**, *23*, 1325-1335.

SUPPORTING INFORMATION

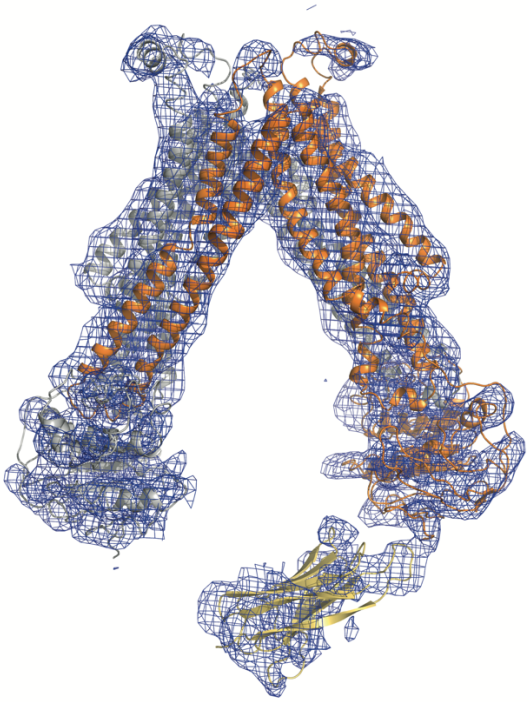

Figure S1. 2Fo-Fc electron density map of PglK-E510Q•Nb93 complex

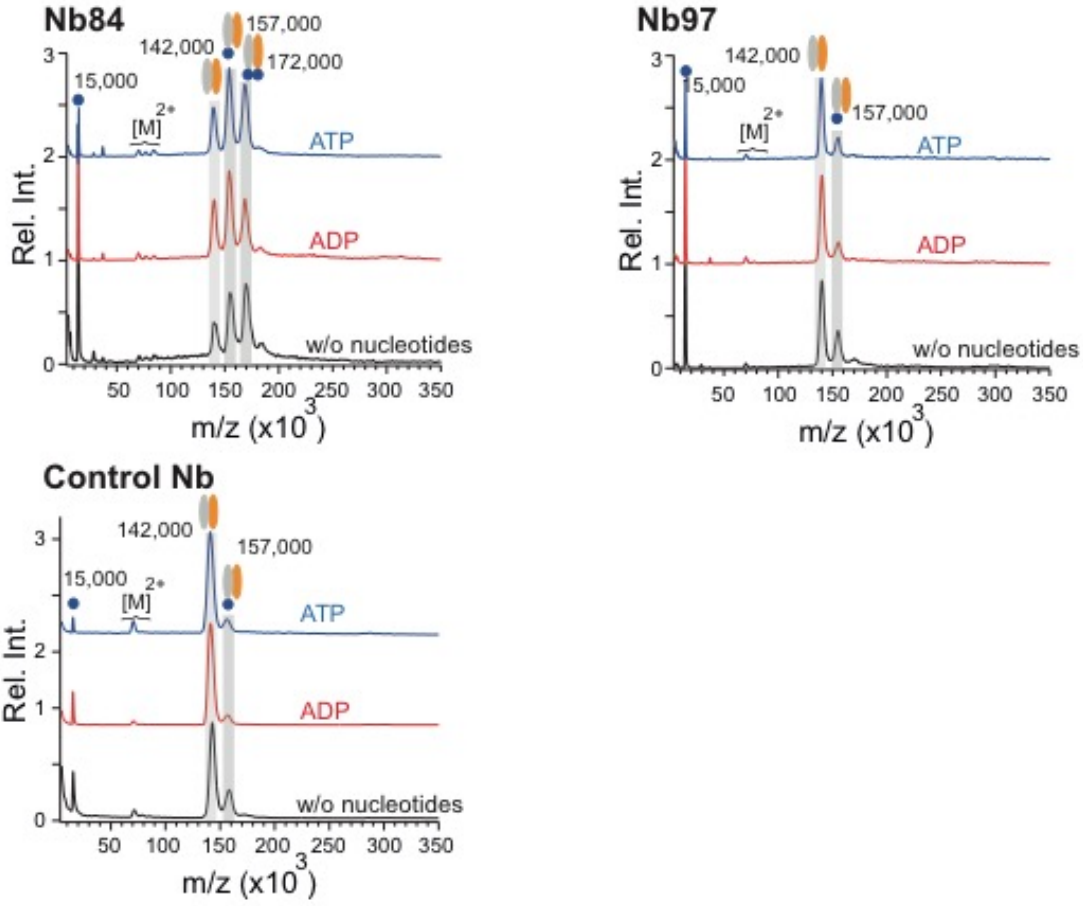

Figure S2. The complex formation of Nb84, 97 and control Nb were observed via MADLI-MS in presence of ADP or ATP, respectively (ADP red trace, ATP blue trace) and compared without nucleotides (black trace). No change in complex formation could be observed. Control Nb spectra were reproduced from Perez et al.[5]

Table S1. Binding affinities, signal-to-noise ratio and root mean square error of reported nanobodies against fluorescently labeled PglK. (-) indicates no fitting detected.

Nanobody	Binding affinity K_D [µM]	Signal-to-noise ratio	RSME
Control Nb	-	-	-
Nb67	-	-	-
Nb84	0.5 ± 0.2	6.34	263.58
Nb87	1.0 ± 0.5	8.54	179.13
Nb93	1.8 ± 1.0	5.64	324.94

Table S2. Fitting parameters for MST-experiment. (-) indicates no fitting detected.

Fitting parameter	Control Nb	Nb67	Nb84	Nb87	Nb93	Nb97
Bound	-	-	7634.5	6450.1	7429.8	5918.8
Unbound	-	-	6074.2	5029.2	5749.2	4288.3
K_D [µM]	-	-	0.5	1.0	1.8	138.9
c_{tar}	500 pM	500 pM	500 pM	500 pM	500 pM	500 pM